https://ntrs.nasa.gov/search.jsp?R=19800006725 2020-03-21T19:30:44+00:00Z

HIGH ENERGY X-RAY RESULTS FROM HEAO-1: X-RAY PULSARS, AND THE ALL SKY SURVEY

Alan Levine
Massachusetts Institute of Technology

I will discuss observations of high energy X-rays that were made with the University of California at San Diego/MIT instrument which was aboard the HEAO-1 spacecraft. Figure 1 shows a top view and a side view of the UCSD/MIT instrument. There were seven detectors in the instrument, five of which were sensitive to low energy gamma rays. Jim Matteson will discuss the results from those detectors. There were also two detectors which were sensitive to high energy X-rays. Each of these detectors contained a slat collimator to define the field of view. X-rays which pass through a collimator are absorbed in a sodium iodide crystal which converts the energy of each X-ray to a pulse of light which is then detected in a photomultiplier at the aft end of the instrument. The fields of view of these detectors are each 1.2 × 23 degrees full width at half maximum. Note that the long direction of the fields of view were each tilted 30 degrees with respect to the perpendicular to the scan direction of the spacecraft. Figure 2 shows the full width fields of view of the high energy X-ray detectors and the scan plane for this particular orientation of the satellite projected on the celestial sphere.

Also shown in Figure 2 are the X-ray sources from the 4U catalog. In fact, hundreds of X-ray sources have been detected in the energy range 2 to 10 keV, the canonical energy range for X-ray astronomical observations. The spectrum of the typical galactic source is thermal with an exponential shape corresponding to a temperature of about 5 keV. If one extrapolates a spectrum such as this up into the energy range of the UCSD/MIT instrument, the typical source fluxes integrated over energy bands of interest are about 1000 times lower than in the 2 to 10 keV band. Therefore, if we were to have a detector that could detect the faintest sources with this spectral shape that an instrument like HEAO A-2 could detect, then we would need an enormous detector of approximately 1 km^2 in area. However, this is not necessary because there are a lot of sources, such as the Crab Nebula, that do not have typical thermal spectra but have nonthermal spectra. These sources are very apparent and outstanding at our energy range and also tend to be among the most interesting sources in the sky.

The first topic will be the results of our sky survey with the high energy X-ray detectors of the A-4 experiment aboard the HEAO-1 spacecraft. The sky survey is the result of analysis of scanning data from the mission and, to make the presentation clear, we need to explain the mode of operation of the satellite during scanning (Fig. 3). During scanning, the spin axis, which is designated as the Z-axis, of the

satellite is always pointed toward the Sun. Therefore, all possible satellite orientations of spacecraft during scanning can be labeled with two coordinates. We have chosen one of these coordinates to be the ecliptic longitude of the Z-axis of the spacecraft and the other coordinate to be the azimuth of the Y-axis around the Z-axis. The north ecliptic pole is defined as the origin of the azimuth coordinate.

Figure 4 shows the fields of view pointing along the Y-axis of the spacecraft. Since we have long, narrow tilted fields of view, a high energy X-ray source which is not on the scan plane on a given day will be seen at different azimuths in the two detectors. As days go by, the scan plane will move and the azimuth at which the source is seen in each detector will change. When the scan plane crosses over the X-ray source, it will be seen at the same azimuth in both detectors.

Results from both detectors are plotted in Figure 5. What we see plotted is the average count rate of each detector averaged over all time at each possible satellite orientation. The vertical coordinate is the Z-axis ecliptic longitude; the horizontal coordinate is the Y-axis azimuth; the average count rate is encoded in intensity. Most of the hash is background, but sources, which appear at different azimuths for different Z-axis longitudes, show up as dark tilted stripes. These data cover the whole energy range from 13 to 80 keV. The bright sources which are evident include the Crab Nebula, 4U0900-40, Cen X-3, Cen A, and Sco X-1. A large number of sources near the galactic plane in the galactic center region are also evident. Sources in the Cygnus region are Cygnus X-1, X-2, X-3, and 4U0115+63. Note that the sources are tilted at different senses in the two detectors.

In Figure 6 we see data from one of the detectors in two more restricted energy ranges. The energy range of the data in the top panel is 13 to 25 keV and in the bottom panel is 25 to 40 keV. So far, by visual inspection of these data, which cover the first 6 months of the mission (2700 orbits of data), we can see about 40 sources above 13 keV and about 30 sources in the energy band of 25 to 40 keV. Immediately, one can notice spectral variations among the sources. For example, Cygnus X-2, which is prominent below 25 keV, disappears above 25 keV.

In Figure 7 we proceed to higher energy — 40 to 80 keV. This is data for the same detector. Again by visual inspection, we see approximately 15 sources above 40 keV. In fact, about five of those are still visible above 80 keV. The sources that are visible include the Crab Nebula, 4U0900-40, Cen A, and GX 339-4 — the black hole candidate which a number of other people have discussed at this meeting. Another of the sources is 4U1700-37, and also shown are Cygnus X-1 (extremely bright) and Cygnus X-3. Preliminary analysis indicates that the emission close to the galactic center must be due to at least five sources. The usually dominant hard X-ray source in the galactic center is GX 1+4, but it is by no means dominant in these data.

Since these data came from the beginning of the mission, Nova Ophiuchi 1977 was bright and, most likely, one of the strongest sources making up this hard X-ray emission. In fact, there is an indication that we detected it above 80 keV indicating that it did indeed have a hard spectrum. It is also likely that there are one or two sources whose location must be within one degree of the galactic center. We are still working on trying to precisely identify the other sources. Source confusion is a problem as one might well imagine.

There are a number of things which we would like to do with these sky survey results. One goal is to make a catalog of X-ray sources and to do that we not only want to identify strong sources (which we do by visual inspection), but to find weak sources in these data. We also want to search for time variability. A sample of that is shown in Figure 8. This is a blow-up of the 13 to 25 keV band for one detector of the region around 4U0900-40. Since the Z-axis moves uniformly around the sky with the Sun, we can interpret Z-axis ecliptic longitudes as a crude time coordinate as well. The horizontal lines are spaced at 5 degrees in ecliptic longitude and are, therefore, 5 days apart. We see a modulation in the intensity of 4U0900-40 due to the eclipses which occur every 9 days. Time variability is seen as well in a number of other sources.

The last thing we want to do is determine crude spectral parameters for a large number of these sources. One technique we have for finding weak sources is demonstrated in Figure 9. As previously mentioned, we can only find strong sources by visual inspection in our sky maps, so we perform azimuthal superpositions to look for weak sources. Note that sources stand out by visual inspection in the sky maps only if they are the equivalent of about 8 sigma or greater in statistical significance (for a 20-day integration time). Using this technique, we can set a more reasonable number such as four sigma for a detection limit. We have not systematically used this technique to study our data, but intend to do so. Figure 9 shows 20 days of data taken near the beginning of the mission. The scan plane went right over the Crab Nebula, the sharp feature at about 90 degrees. At about 270 degrees is the galactic center region. There is a hint of some emission right around the galactic center region in the 80-180 keV band, but it is only a small fraction of the intensity of the Crab. The emission above 80 keV is probably due to a superposition of the emission from two or three sources.

When we find all sources detected at the 4 sigma level of significance instead of the 6 or 8 sigma which was the detectability limit for visual inspection our sky map, and when one more year's worth of scanning data are also analyzed, we hope the number of detections will increase considerably above that which we have preliminarily noted.

We will now turn to our results of studies of X-ray pulsars. First, let us provide a brief description of an X-ray pulsar in terms of current theory. Figure 10 shows a neutron star of black hole, which is a

massive (roughly a solar mass) compact object, orbiting around a normal star. Matter from the envelope of the normal star is drawn towards the neutron star, spirals around it in an accretion disc and falls into the gravitational potential well of the neutron star. The energy released in the infall of this matter heats the infalling matter to very high temperatures, on the order of a hundred million degrees Kelvin. It, therefore, profusely emits X-rays on its way down. Figure 11 shows that the matter is confined to fall down toward the magnetic poles of the neutron star because of the presence of an extremely intense magnetic field. Thus, the X-ray emission will have an intensity which varies with direction. A pulse is observed since the neutron star is spinning about an axis and the magnetic axis is not co-aligned with that spin axis. With this theory, one can identify the pulse period of an X-ray pulsar with the spin period of a neutron star.

Figure 12 shows the pulse profile of the X-ray source 4U1626-67, in the energy range 19 to 30 keV. The energy dependence of the pulse shape is examined in Figure 13. Notice how rapidly the pulse shape varies as a function of energy. Another object which shows behavior similar to that, in that the pulse shape changes as a function of energy, is the X-ray pulsar GX 1+4, whose pulse profile is shown in Figure 14. Whereas 4U1626-67 has a period of 7 sec, the period of GX 1+4 is 116 sec. Notice the sharp spike at the top of the maximum.

An object with quite different behavior is 4U0115+63, for which in Figure 15 we show a composite light curve in the 12 to 66 keV band. The pulse period of this object is 3.6 sec. We can also examine the pulse profile of this object as a function of energy. In contrast to 4U1626-67 and GX1+4, Figure 16 illustrates that the pulse shape apparently is independent of energy between 13 and 30 keV. However, the amplitude of this pulse does not seem to be independent of energy. The pulse is strong at low energies. It seems to be pretty weak around 20 keV and is strong again at the top of the energy range.

Pulsed and unpulsed spectra as a function of energy are shown for both detectors in Figure 17. The feature just alluded to is seen as a dip in the pulse amplitude at about 20 keV. The reason it does not show up so strongly in the first detector (LED No. 1) is that this detector does not have as good an energy resolution as LED No. 2. This feature can be interpreted as cyclotron absorption occurring near the neutron star. To understand this in a very general manner, we have to understand the behavior of matter in a magnetic field (Fig. 18). The velocity component parallel to the magnetic field of a charged particle is unaffected by the presence of the field. Therefore let us just study the motion projected on a plane perpendicular to the magnetic field. The motion is circular and the energy levels of the particle are quantized such that the energy is approximately an integer times a constant times the magnetic field strength. For a magnetic field strength

of 10^{12} gauss, these energy levels are separated by 12 keV. If X-rays are traveling through a medium containing ionized gas in a 10^{12} gauss, magnetic field, for example, they will be more strongly absorbed if their energy is just enough to excite an electron an integral number of energy levels, 12, 24, 36 keV, etc. That is the way that a cyclotron absorption line can arise.

HEAO-1 has made quite extensive observations of perhaps the most fascinating X-ray source in the sky, Hercules X-1. The source has a 1.24 sec pulse period. In Figure 19 light curves are shown from different binary phases and different intervals. We note that the pulse shape seems to be independent of both parameters.

Figure 20 is the pulse spectrum which we have obtained for this source and it seems to be the same on at least six different occasions, at least with respect to the analysis which we have performed so far. We do not see any secondary peaks in the profile as reported by the Max Planck Institute from a balloon flight. This shape can be interpreted in any number of ways. It is a complex shape as you can see, it falls steeply, levels off somewhat, and then falls not quite so steeply. It can be fit by a continuum with an emission line at about 50 keV. It must be a broad emission line; a narrow emission line does not fit. It can also be fit with an absorption line in a continuum. It can also be fit by the sum of two continua.

To close, we will just present one additional light curve (Fig. 21). These are light curves from the object which was just discovered to be pulsing by the HEAO A-2 group. It is the 38-sec pulsar. We see it in the 13 to 25, 25 to 40, and 40 to 80 keV channels, but not above 80 keV. Hopefully, we can detect this source in scanning data within the next few weeks, and help to locate its position in the sky which is at present not well known.

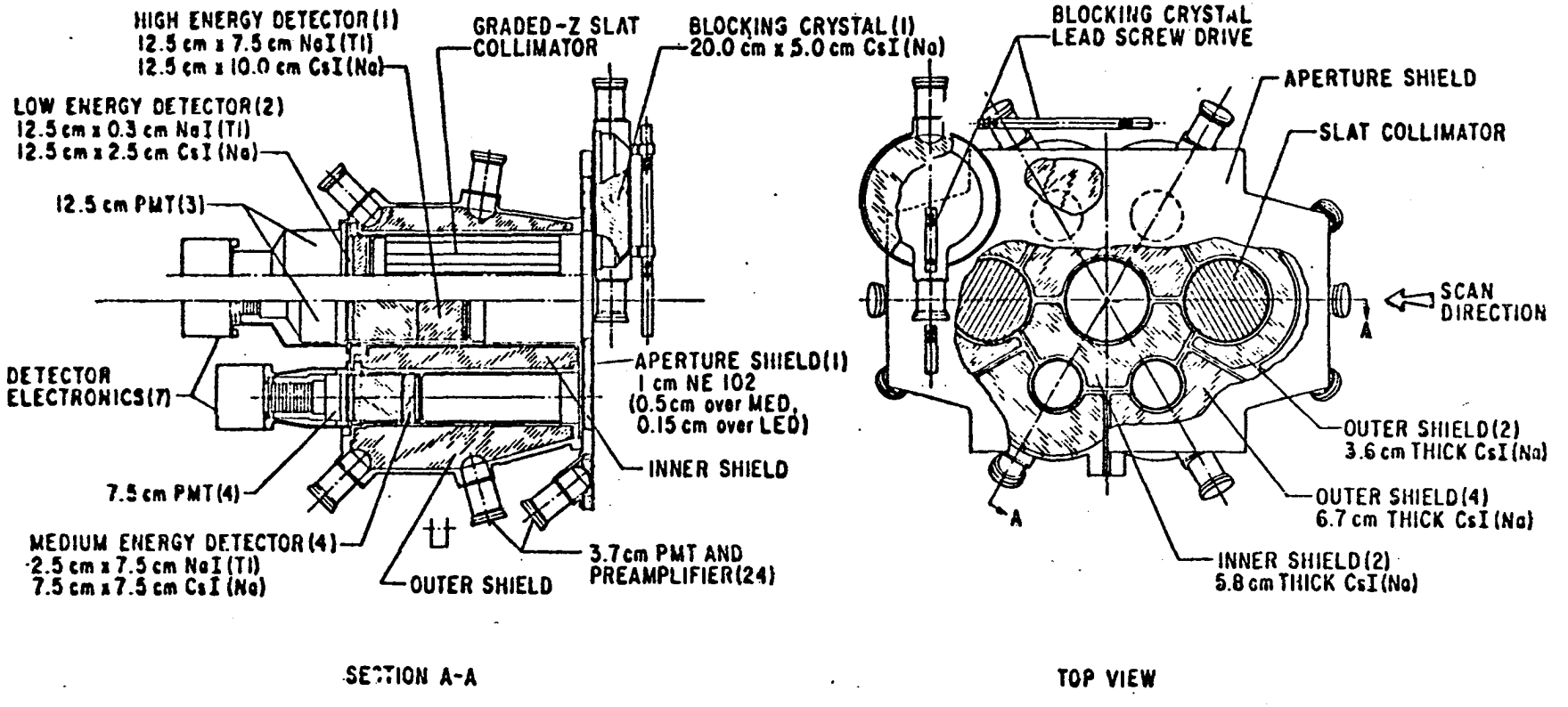

Figure 1. UCSD/MIT High Energy X-ray and Low Energy Gamma Ray Instrument of HEAO-1. Results obtained with the 2 detectors labeled "Low Energy Detector" are discussed in this article. These 2 detectors are behind the slat collimators.

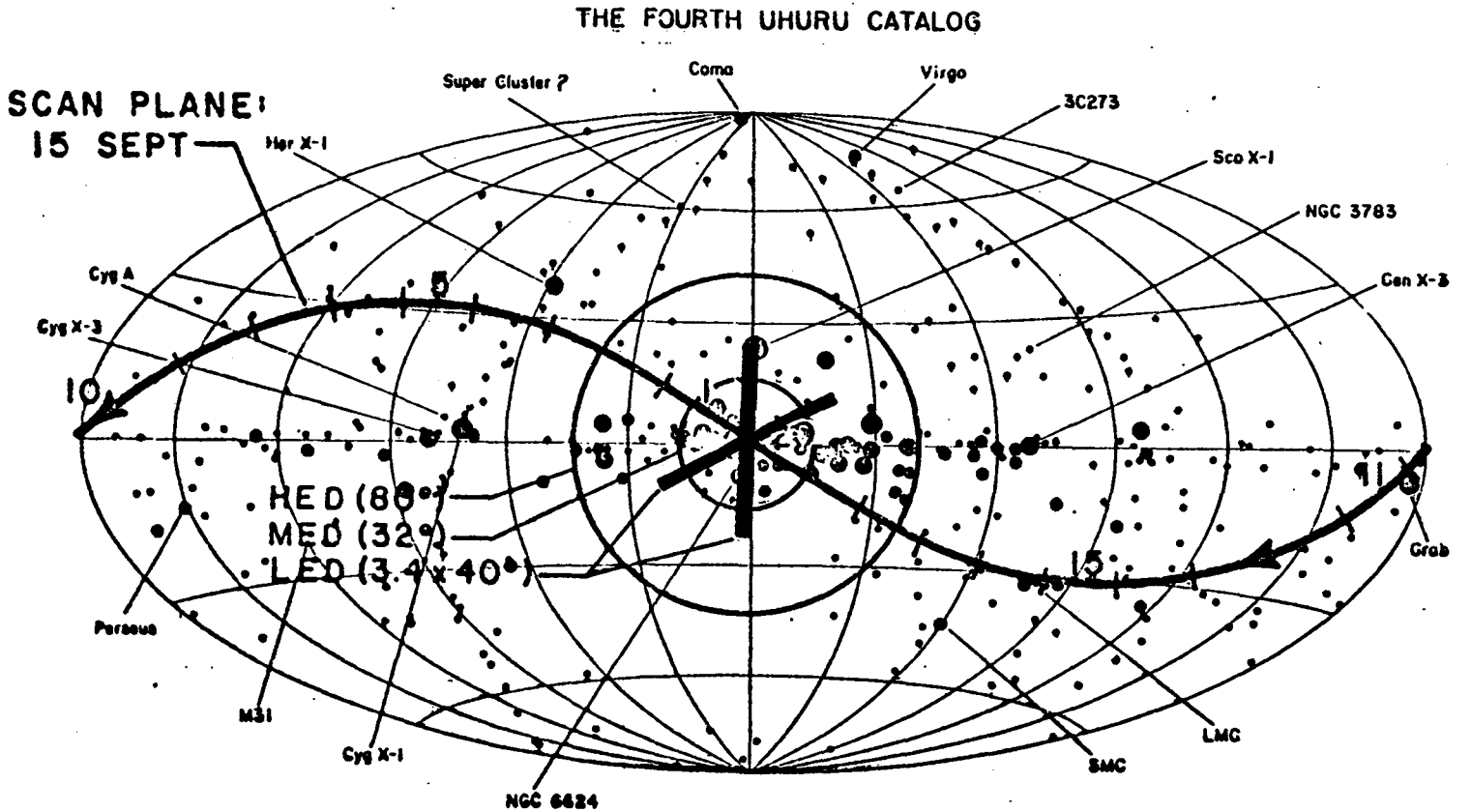

Figure 2. The full width fields of view of the high energy X-ray detectors (labeled LED) are projected onto a map of the celestial sphere in galactic coordinates. The scan plane of the satellite Y-axis for September 15 is indicated as are the X-ray sources listed in the 4U catalog.

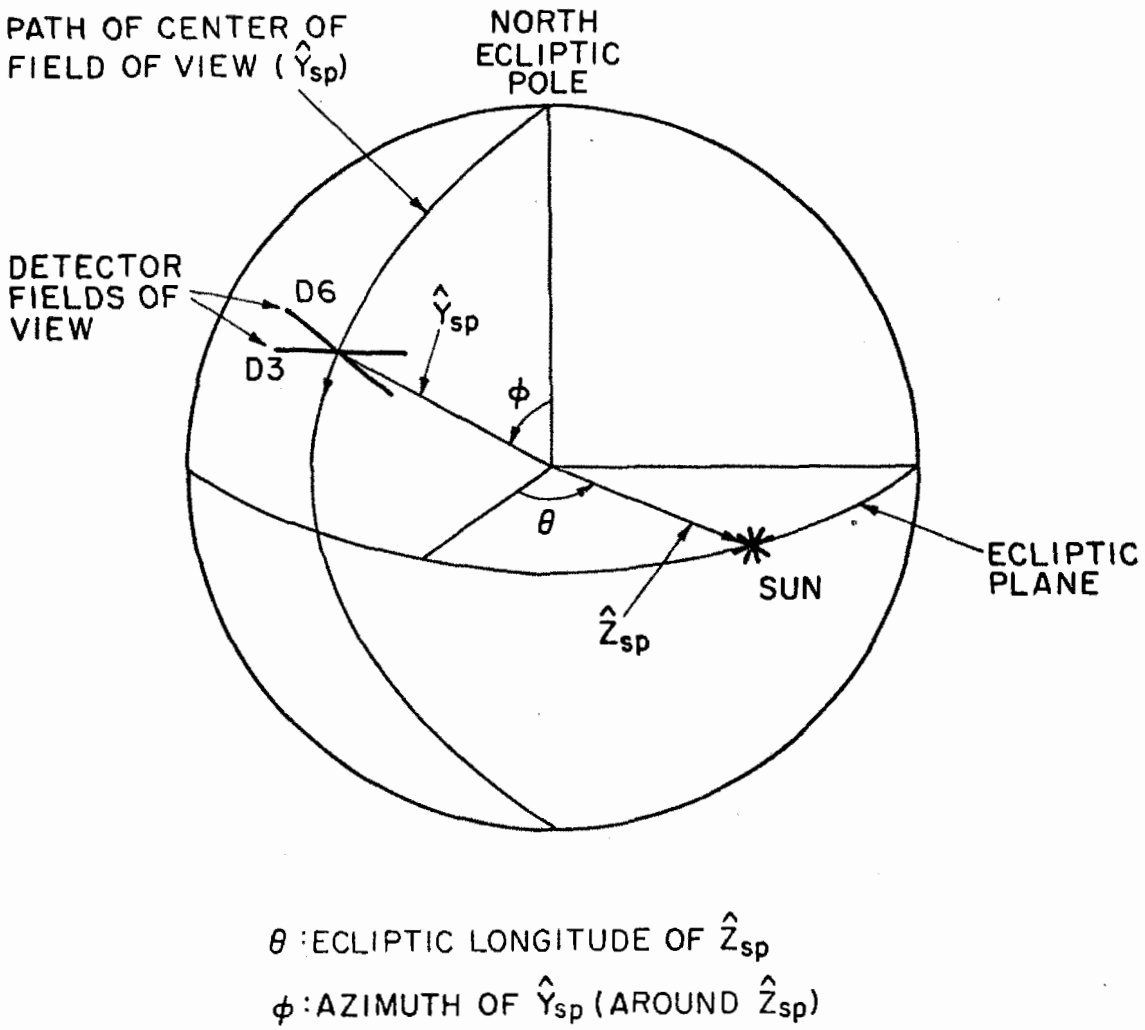

Figure 3. During scanning operations the spin axis ($\hat{Z}$sp) of the satellite was always pointed at the sun. Therefore, the satellite orientation during scanning can be specified using two coordinates. We have chosen as coordinates the ecliptic longitude of the spin axis and the azimuth of the spacecraft Y-axis.

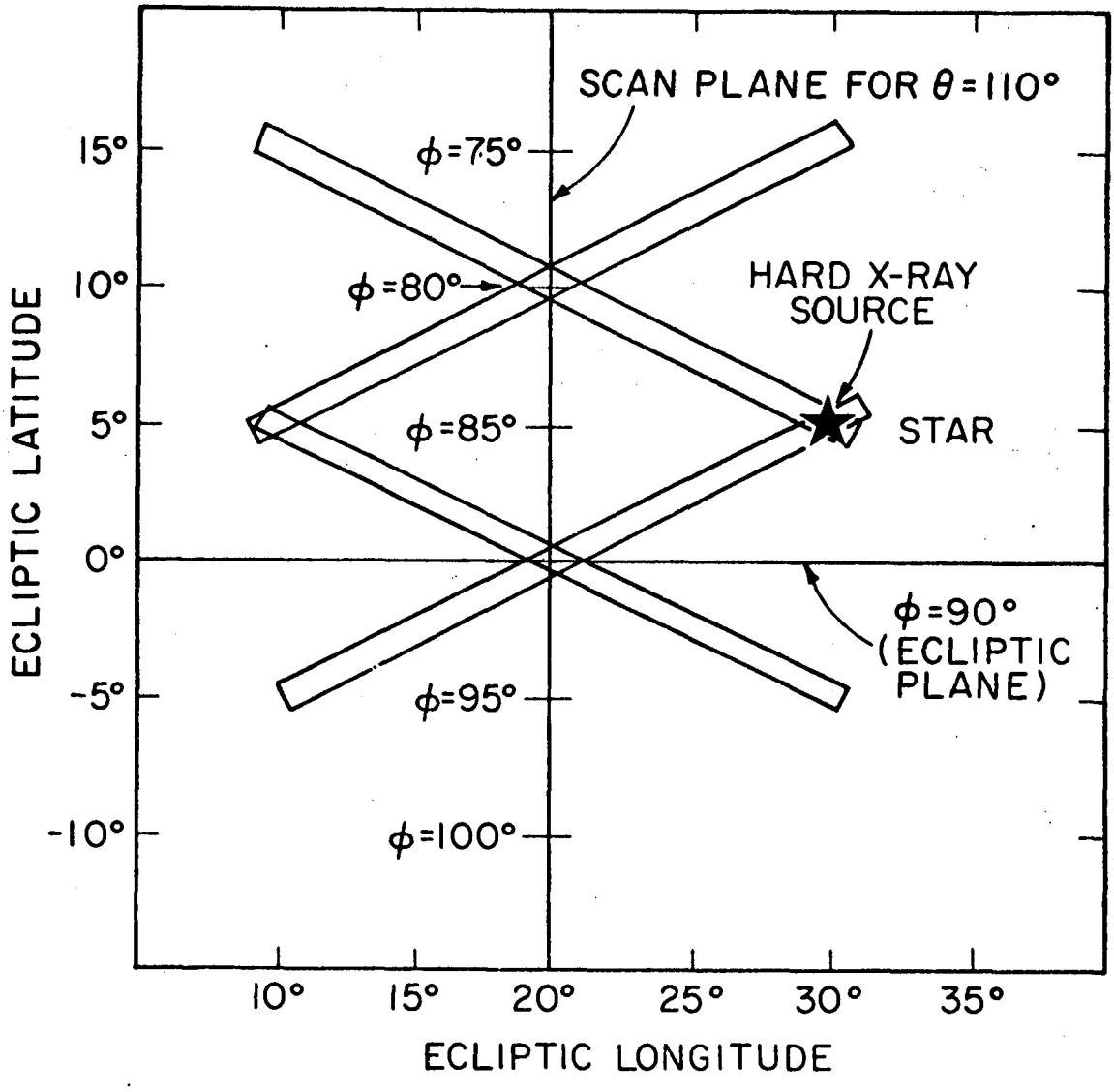

Figure 4. The scan plane for a given spin axis position is projected on a small section of the celestial sphere. The FWHM fields of view of the detectors are shown at the azimuths at which an X-ray source (not on the scan plane) is detected in each of the two detectors. Since the spin axis follows the sun around the sky, the scan plane will change with time. The azimuth at which the source is detected, by a particular detector, will therefore also change with time.

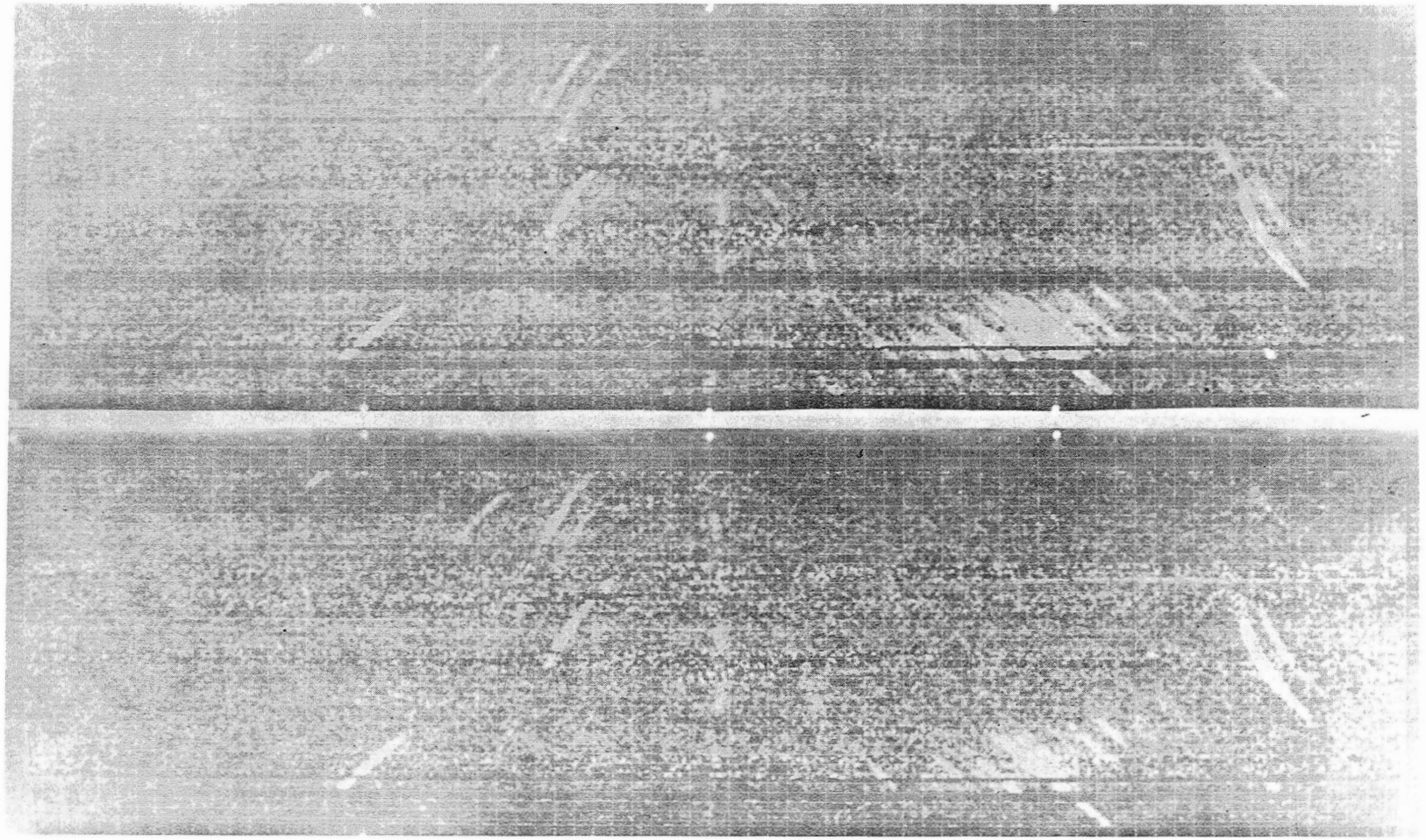

Figure 5. Top: Sky survey results from detector D3. Bottom: Results from detector D6. The average count rate for each possible satellite orientation is encoded as intensity. The satellite orientation is specified by the spin axis recliptic longitude, plotted on the vertical axis, and the azimuth of the Y-axis, plotted horizontally. On a given date the spin axis ecliptic longitude varies little while the Y-axis azimuth covers the entire 360° range. Therefore, data taken on a particular date is represented on a horizontal stripe. The gray background is due both the diffuse X-ray background and non X-ray particle events in the detectors, X-ray sources show up as dark tilted stripes. This data comprises the energy band 13-80 keV.

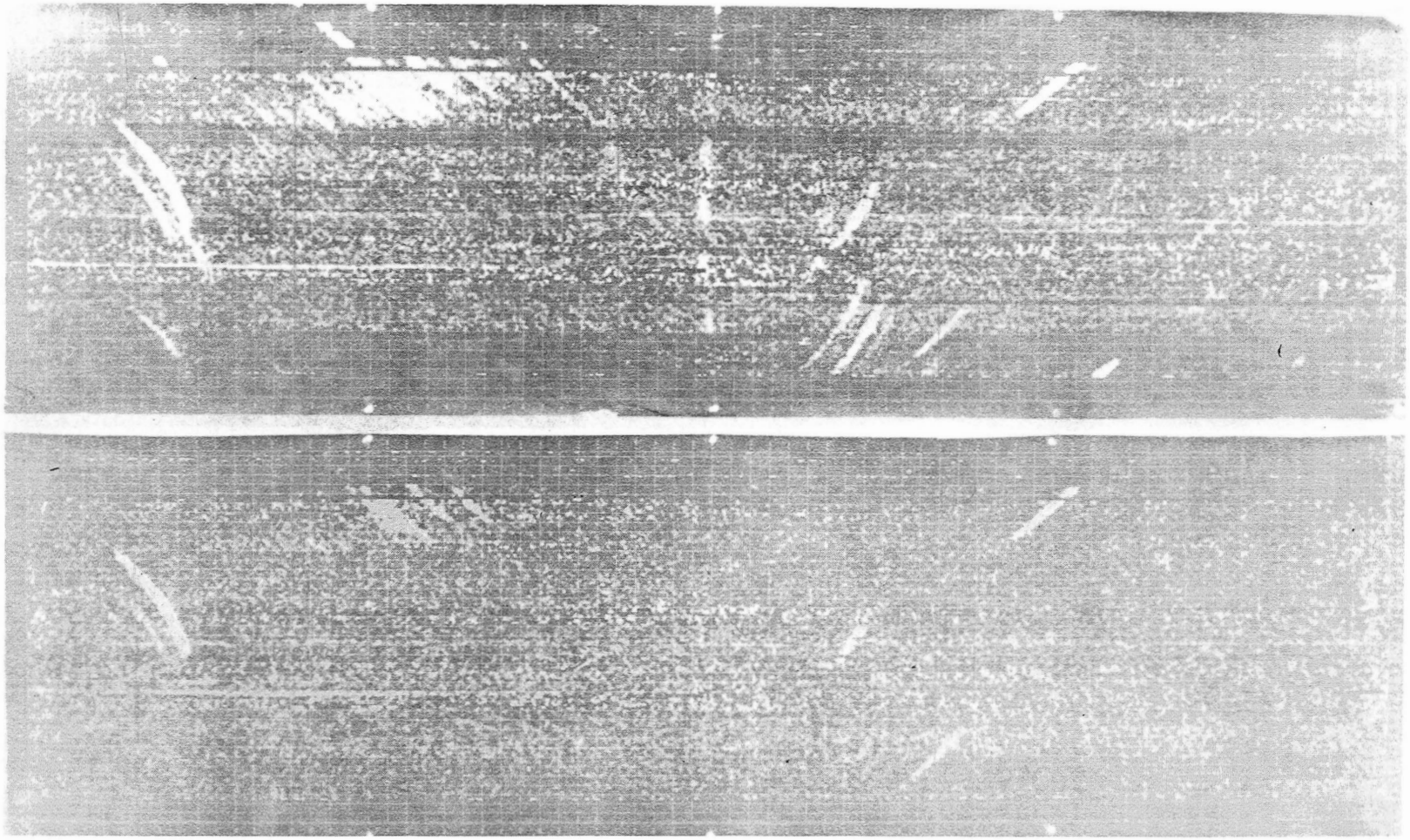

Figure 6. Sky survey results from detector D6 for the energy range 13-25 keV (top) and 25-40 keV (bottom).

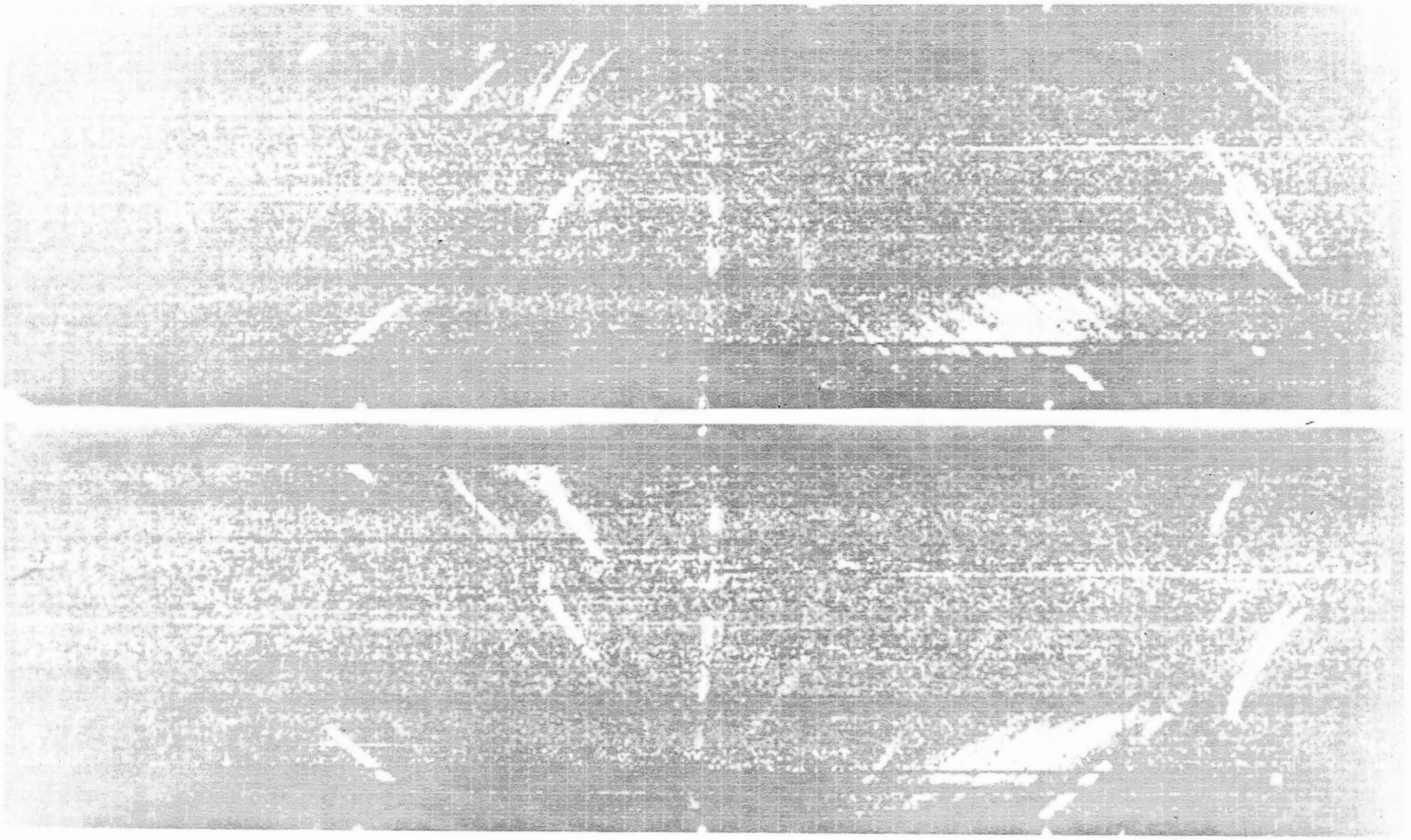

Figure 7. Sky survey results from detector D6 for the energy range 40-80 keV (top) and 13-80 keV (bottom).

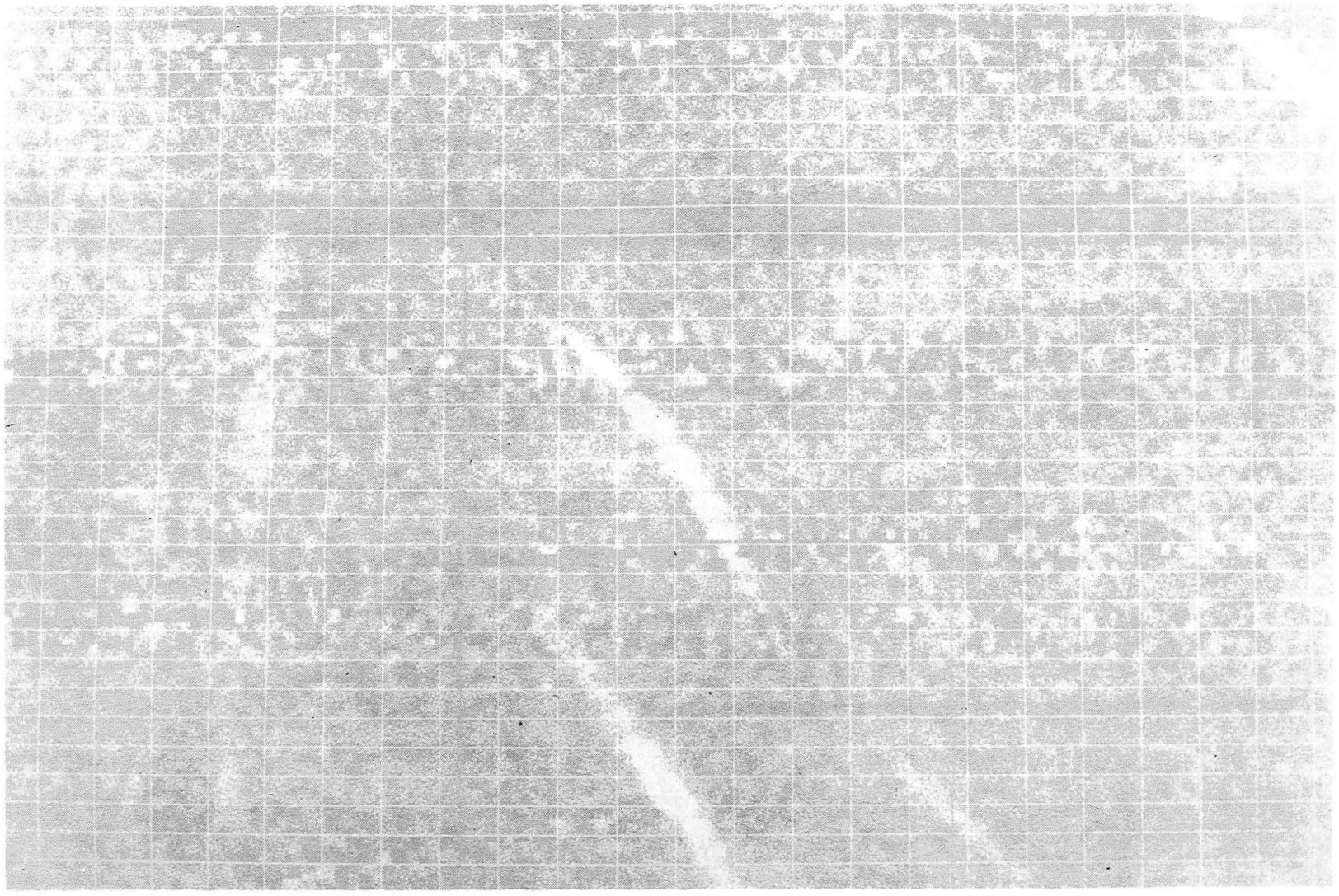

Figure 8. Blowup of the region around 4U0900-40 from Figure 6 (13-25 keV) showing the eclipses occurring every 9 days (see text).

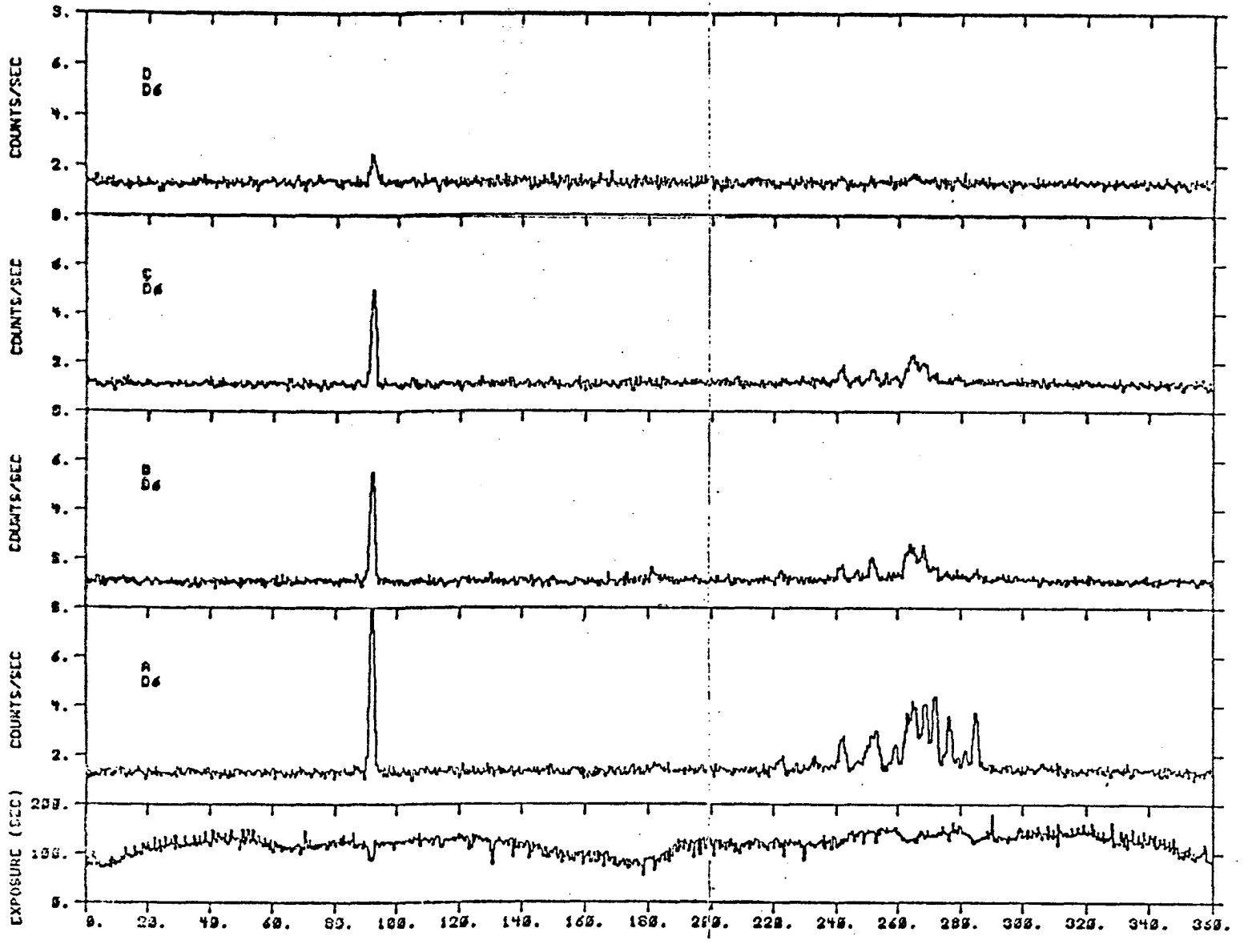

Figure 9. Count rate versus azimuth is shown in each of four energy bands for a superposition of 20 days of data from near the beginning of the HEAO-1 mission. The energy channels are: A, 13-25 keV; B, 25-40 keV; C, 40-80 keV; and D, 80-180 keV. The Crab Nebula is detected near 90° and the galactic center region is viewed near azimuth 270°.

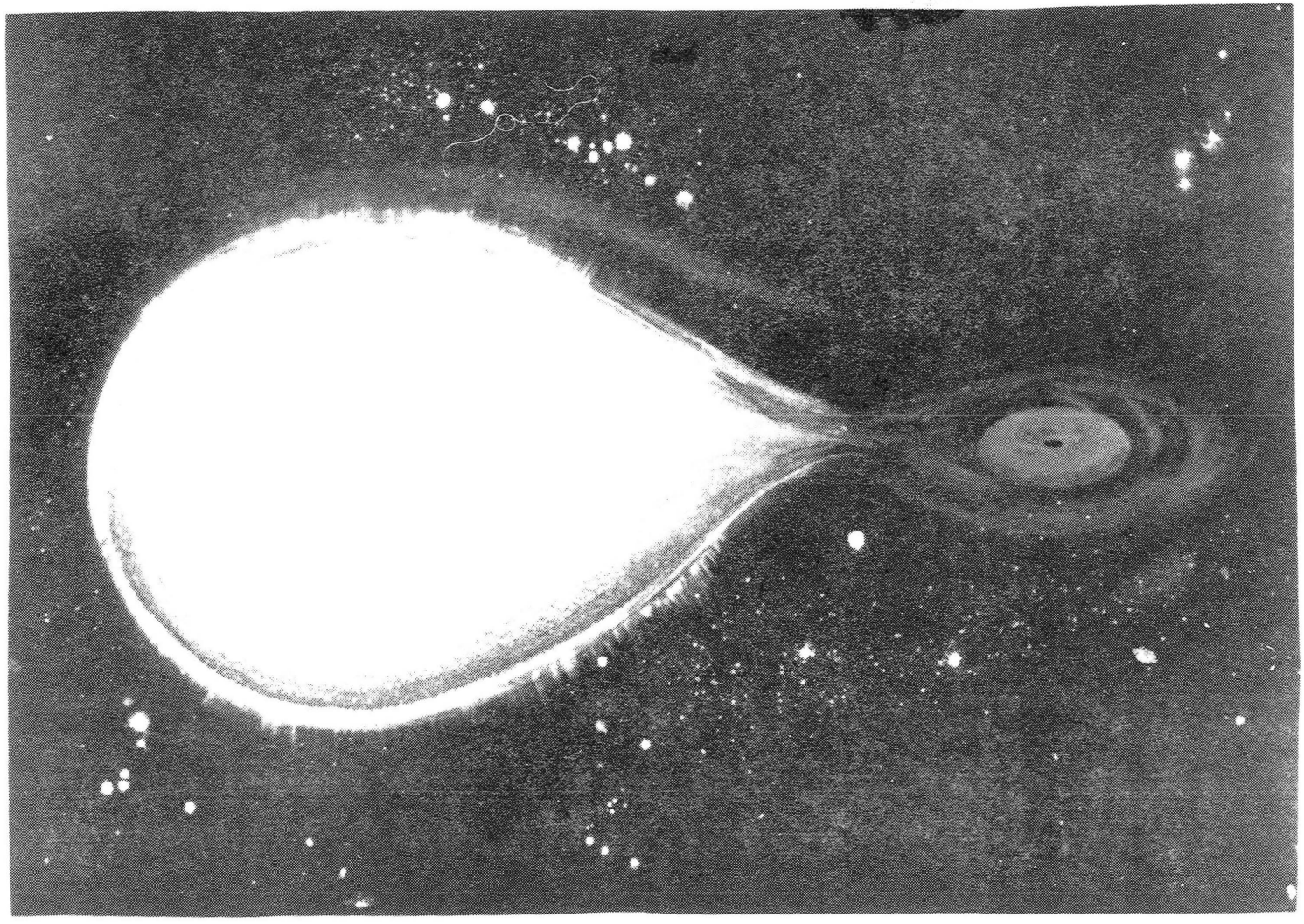

Figure 10. Artist's conception of a binary star system containing an X-ray source. A compact object accretes matter from a normal companion star. This matter forms an accretion disc from which it flows towards the compact object. In the case of X-ray pulsars the compact object is a neutron star. (Painting courtesy Lois Cohen, Griffith Observatory.)

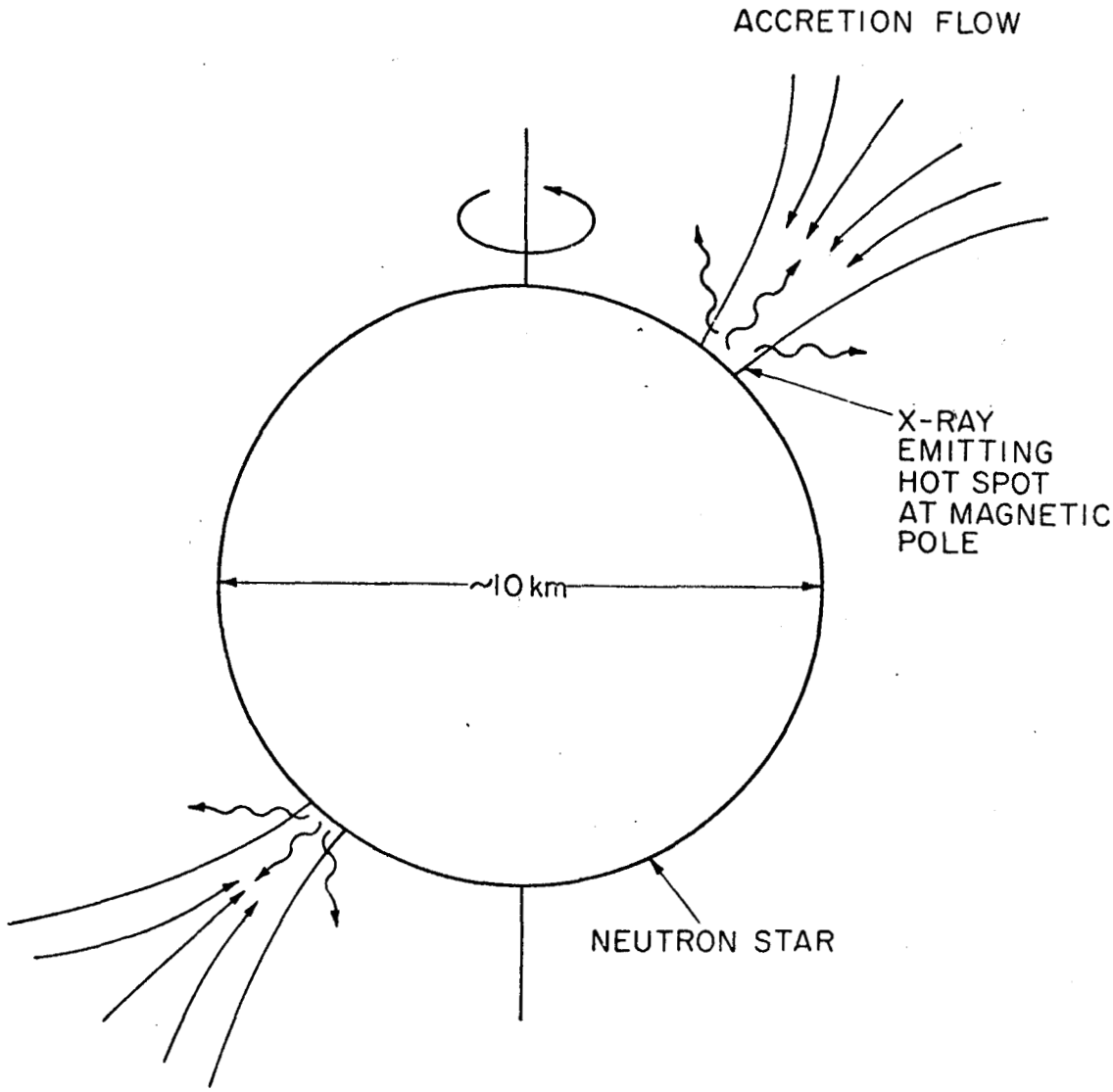

Figure 11. Schematic diagram of an X-ray pulsar. Infalling matter is confined to flow down onto the magnetic poles (which are not coaligned with the rotation axis) of a neutron star. X-rays are emitted anisotropically from hot spots at the bases of the accretion columns. Since the neutron star is spinning, the X-ray intensity varies periodically in any given direction (particularly along the line of sight to the Earth). This is the origin of the observed pulsations.

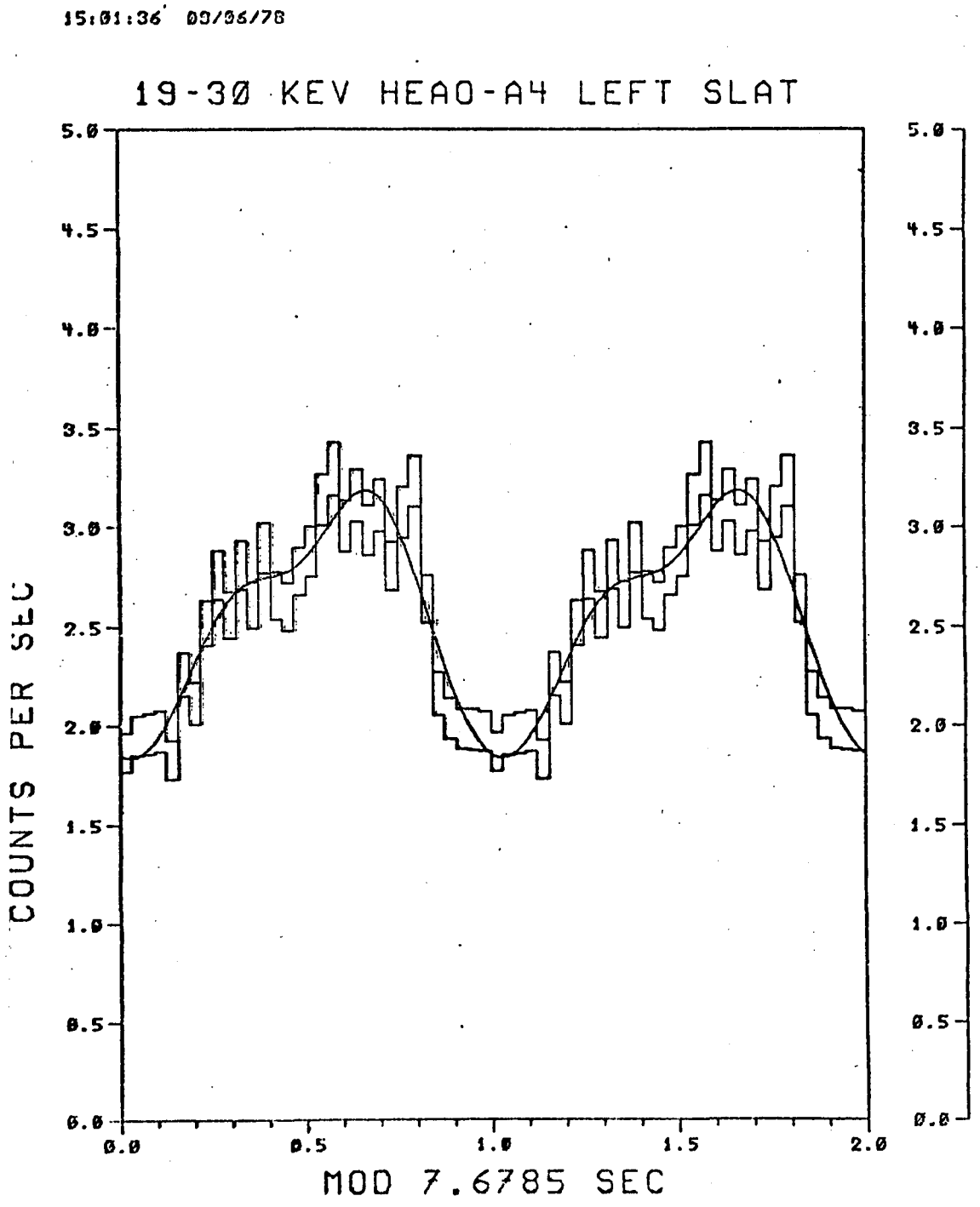

Figure 12. Pulse profile of the X-ray source 4U1626-67 shown in the 19-30 keV energy band. The $\pm 1\sigma$ range of the profile is plotted at each phase. The smooth curve is a fit to the pulse shape. Note that the pulse is plotted twice for clarity.

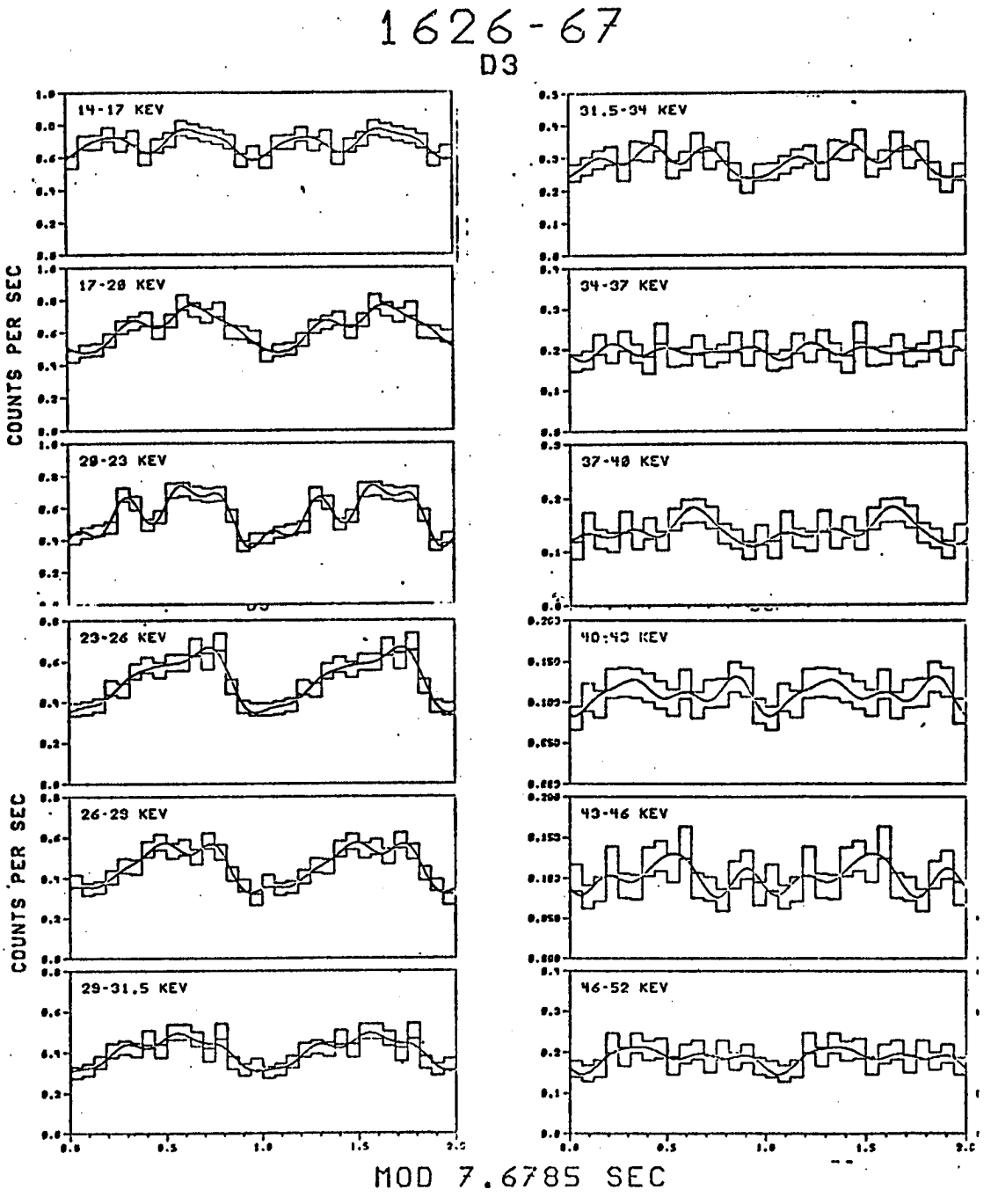

Figure 13. Pulse profile of 4U1626-67 as a function of energy. The shape of the pulse changes rapidly with energy.

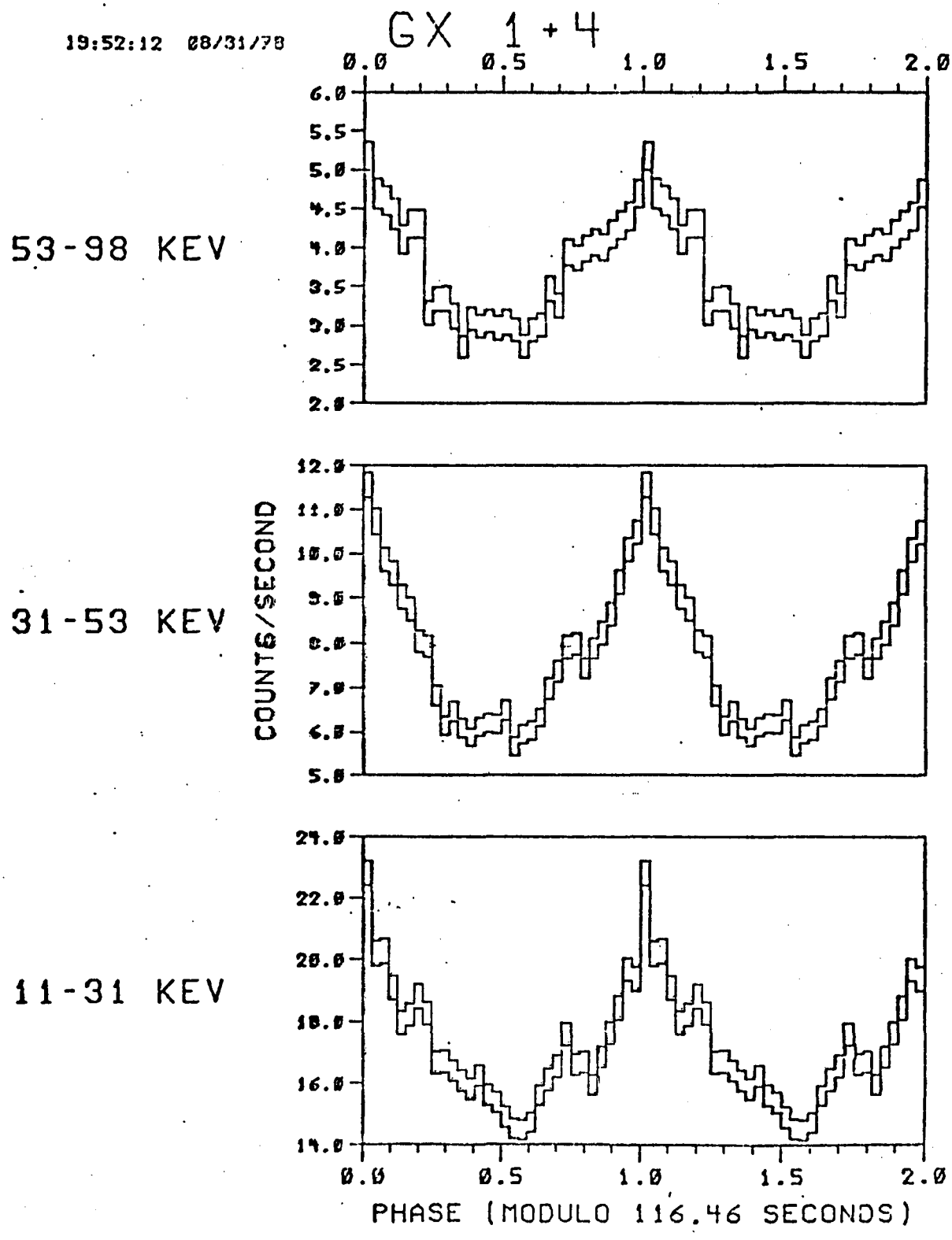

Figure 14. Pulse profile of GX1+4 for each of three energy bands. The shape of the profile of this pulsar also changes with energy.

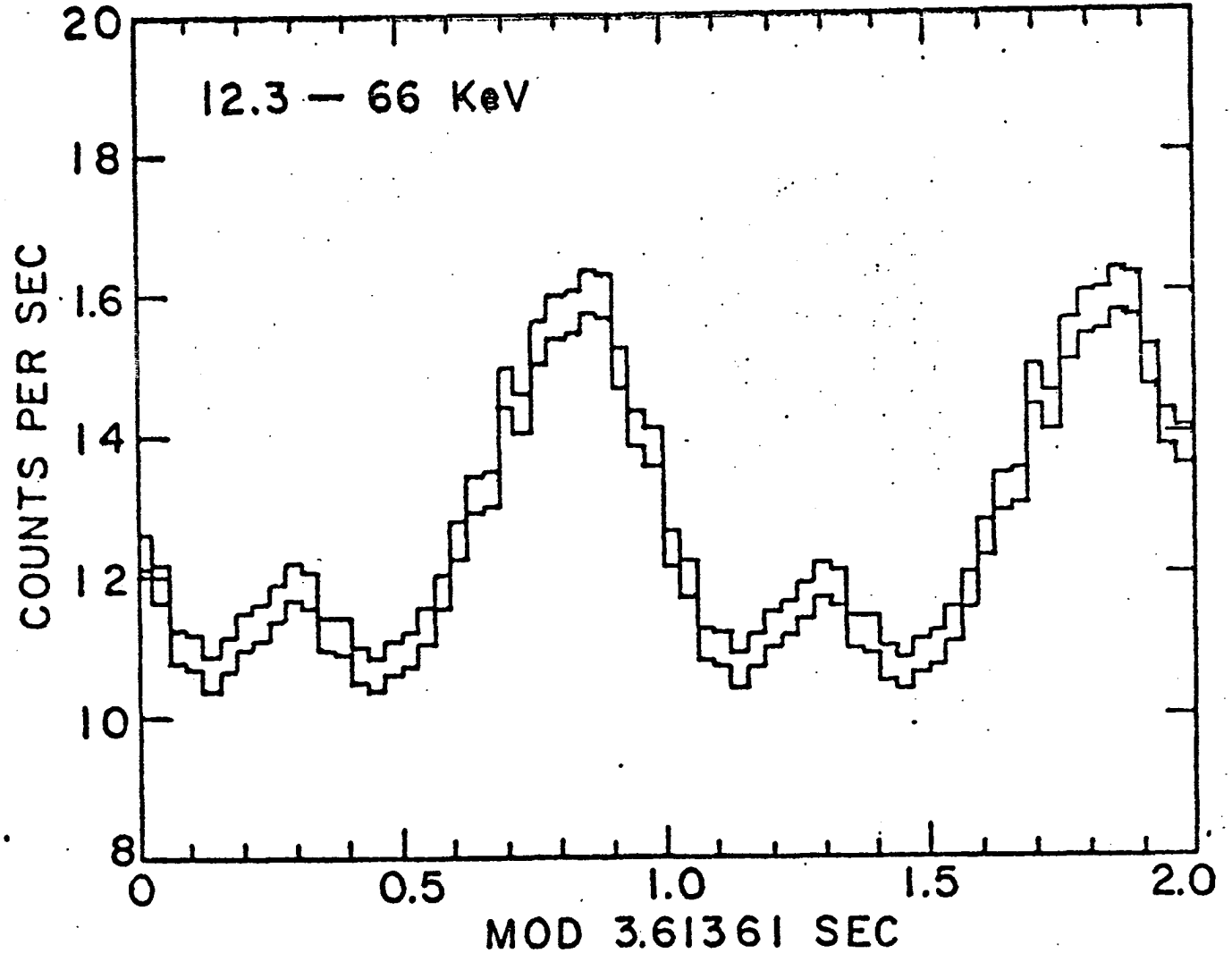

Figure 15. The pulse profile of 4U0115+63 in the energy range 12.3-66 keV.

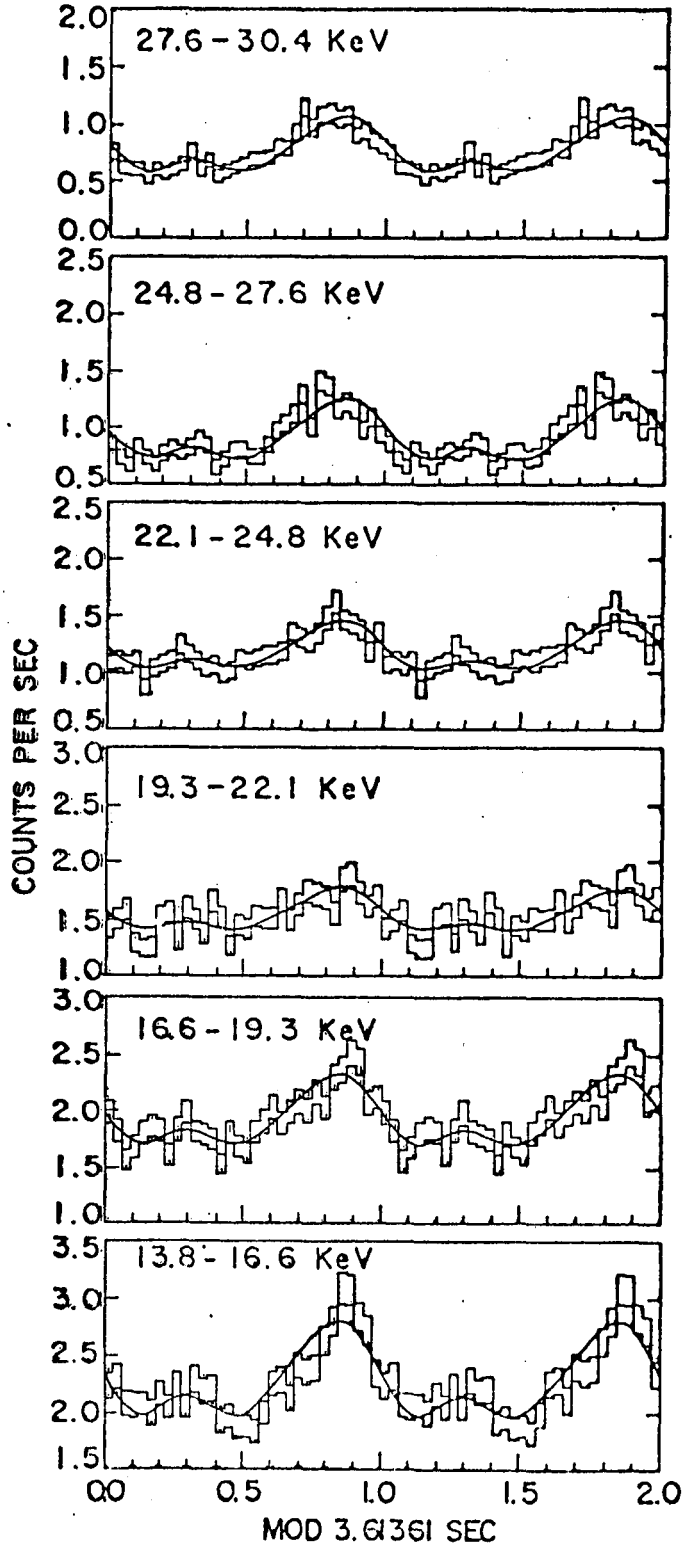

Figure 16. Energy dependence of the pulse profile of 4U0115+63. The pulse shape is independent of energy but the amplitude is not. The pulse is strong at low and high energies and is weak around 20 keV.

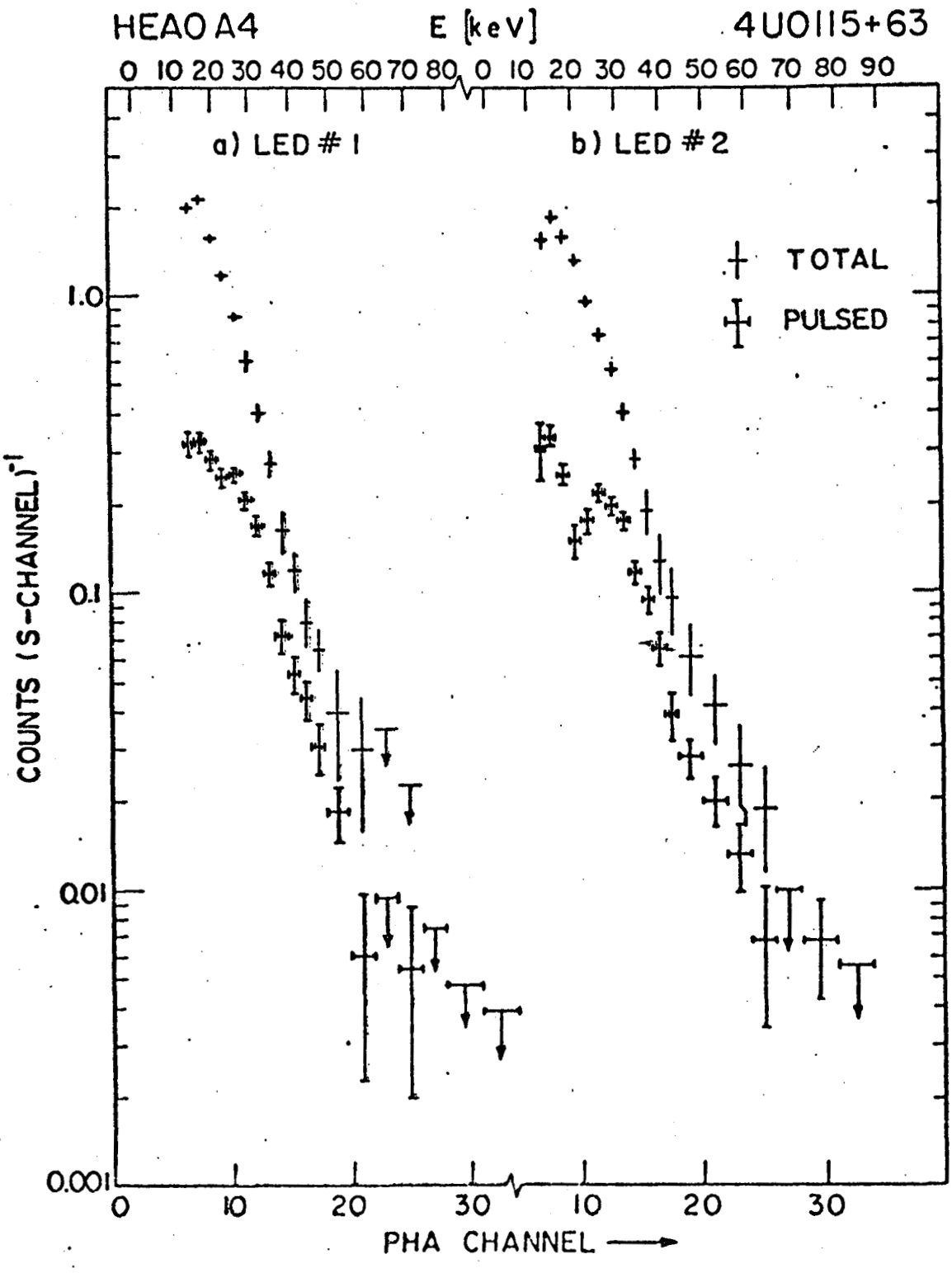

Figure 17. Total and pulsed spectra for 4U0115+63 for both detectors D3 (LED #1) and D6 (LED #2). The dip in pulse strength at approximately 20 keV is clearly evident in the pulsed spectrum from detector D6. The dip is not so evident in data from detector D3 because of inferior energy resolution.

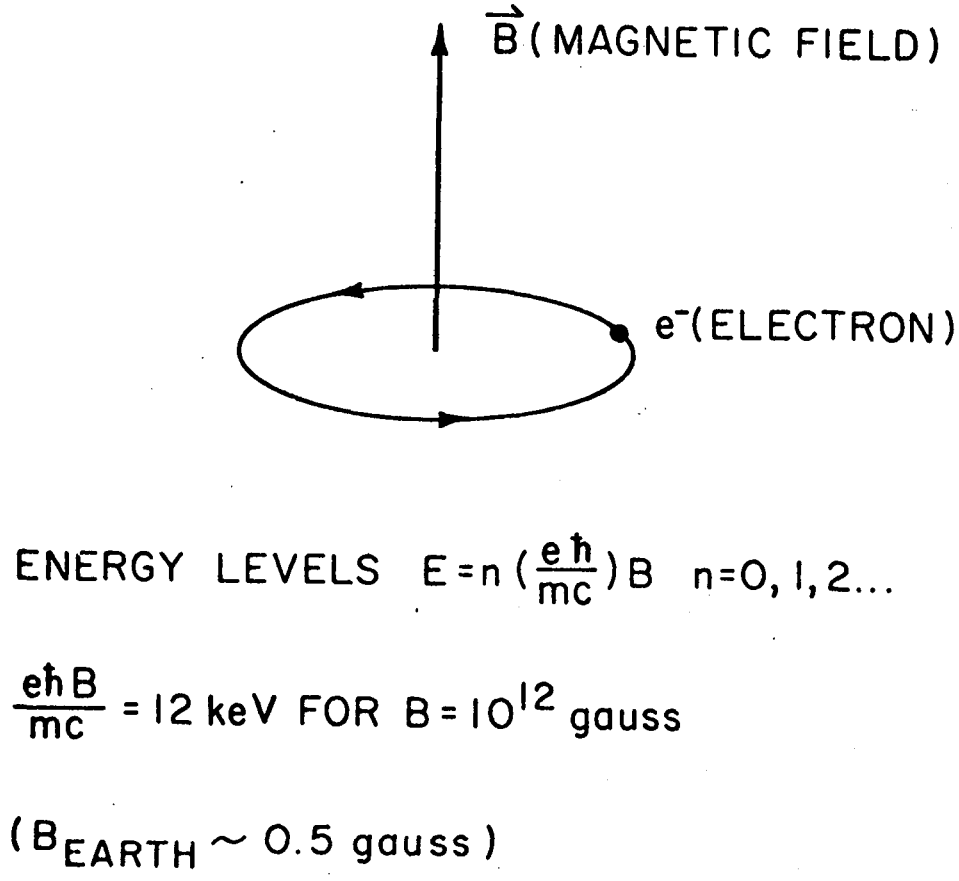

Figure 18. Schematic representation of the motion of an electron in a magnetic field. The velocity component parallel to the magnetic field is unaffected by the presence of the field. The motion perpendicular to the field is circular and the energy levels are quantized. The magnetic field strength near the surface of a neutron star is expected to be of the order of 10^{12} gauss.

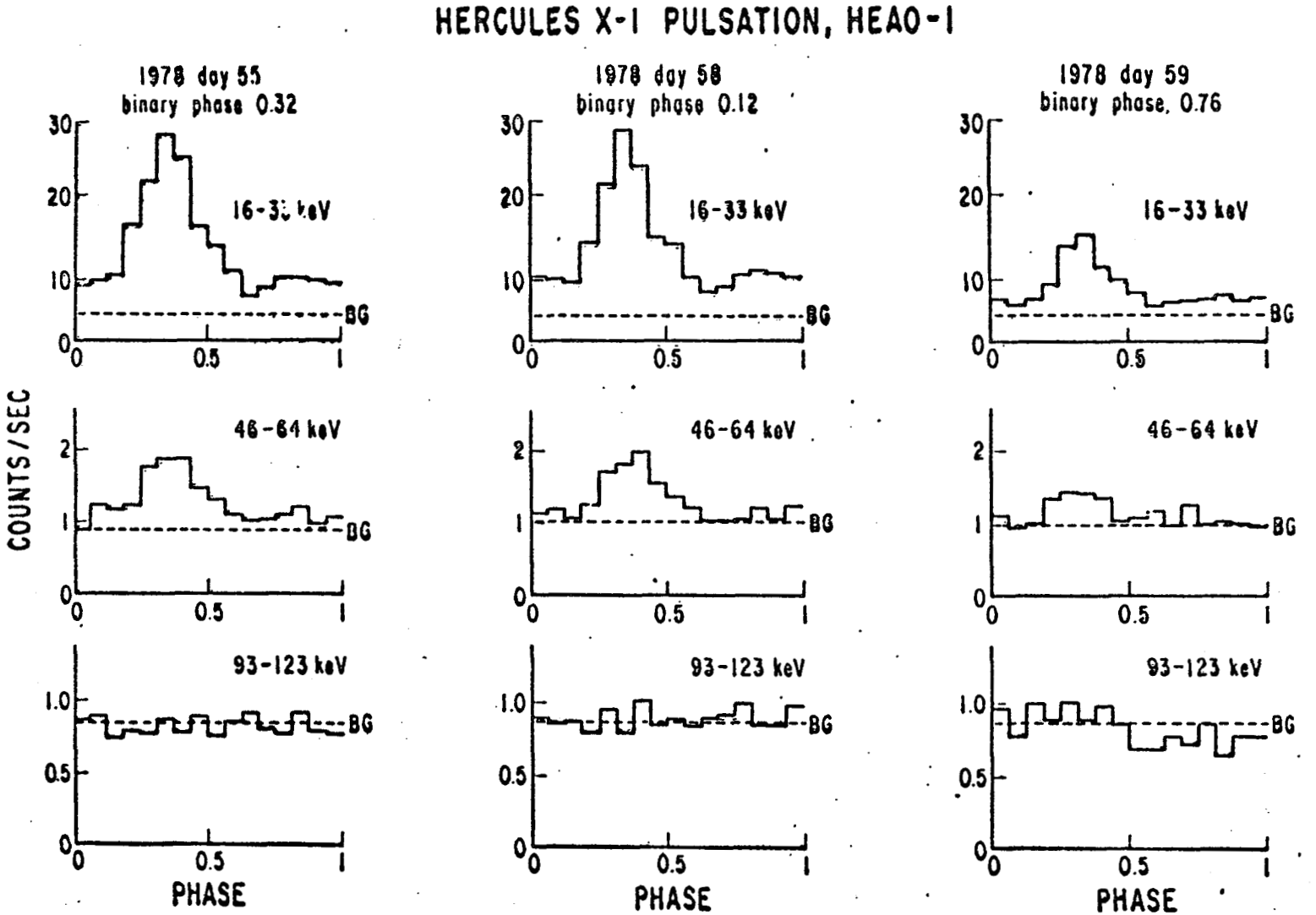

Figure 19. Pulse profiles for Hercules X-1 as a function of energy and binary phase. The shape of the pulse is seen to be constant within the accuracy of the presented data. The pulse period of Hercules X-1 is 1.24 seconds.

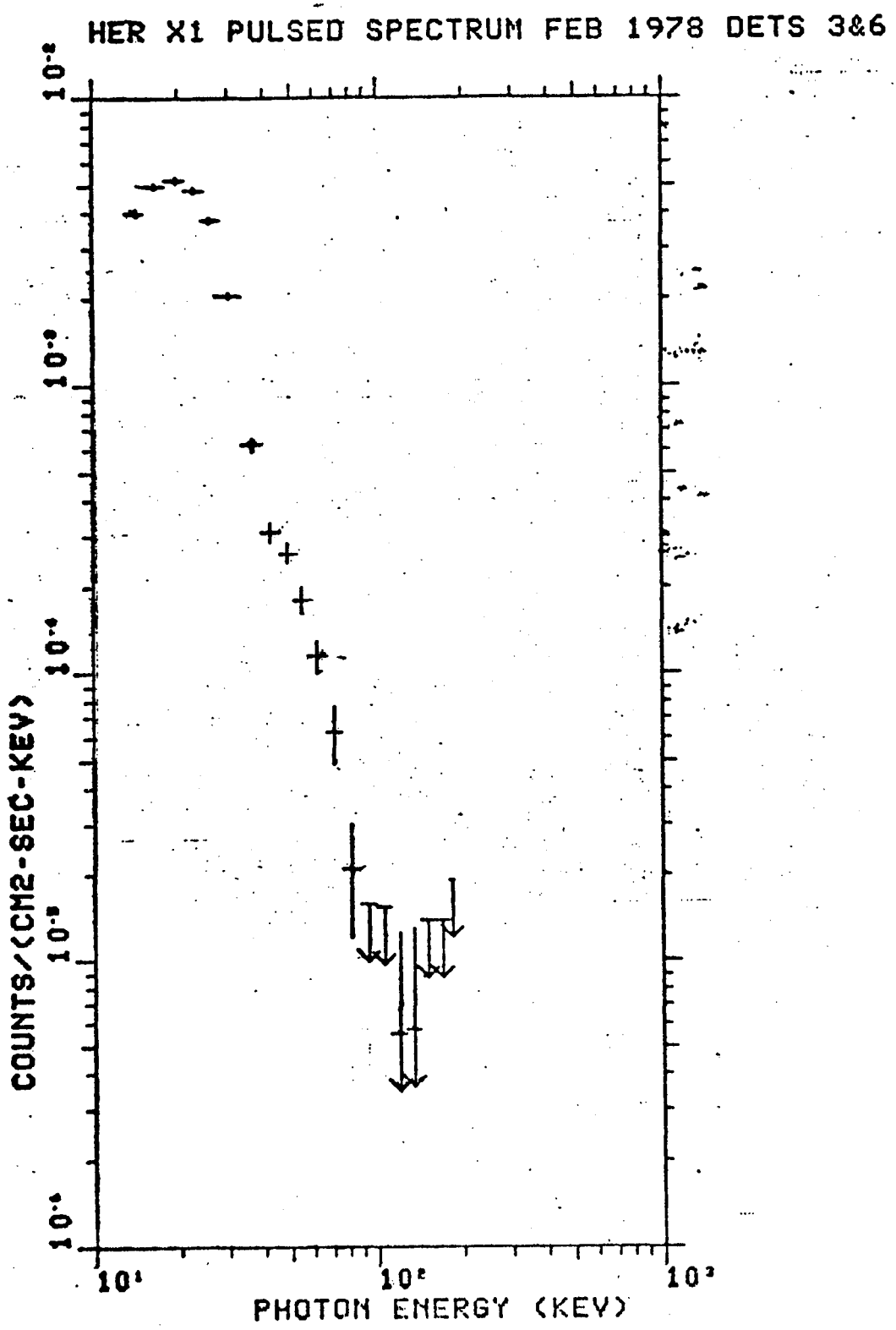

Figure 20. Amplitude of the Hercules X-1 pulse as a function of X-ray energy for the observations of February 1978. Data from both detectors are included.

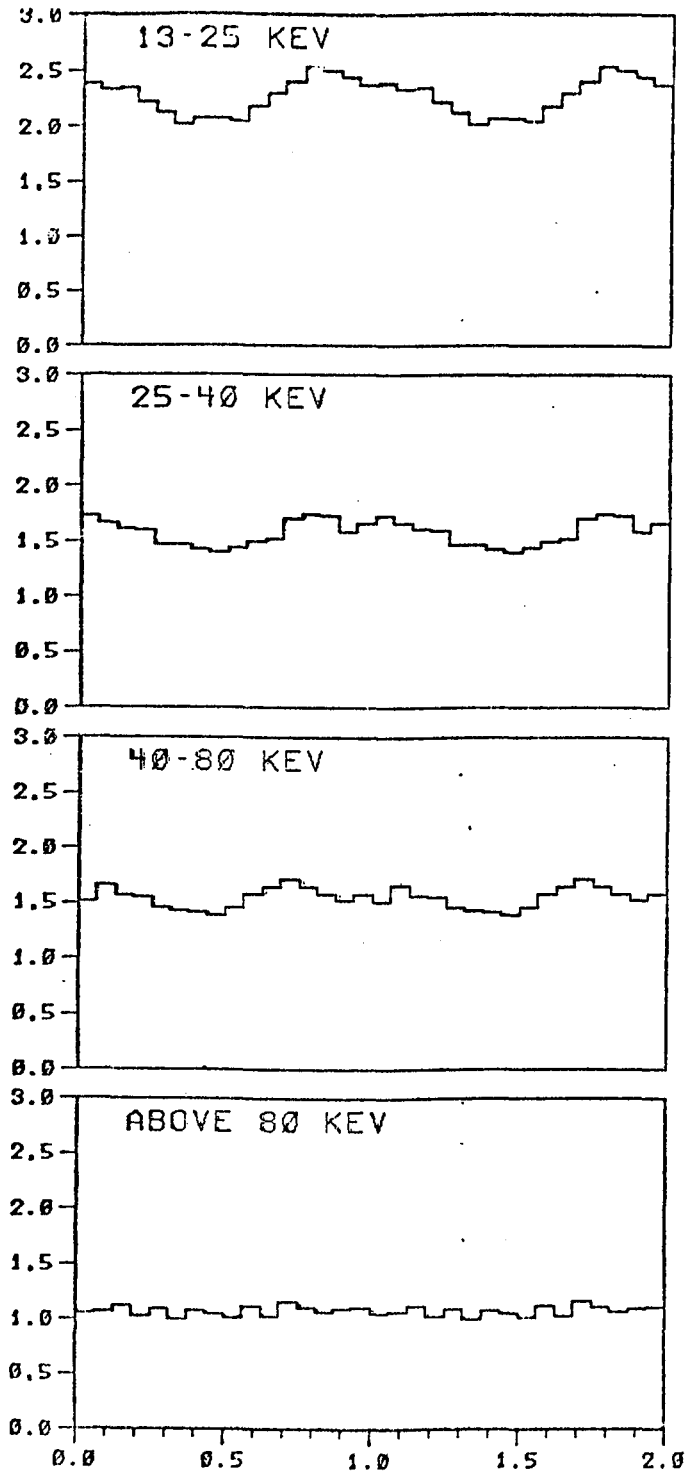

Figure 21. Pulse profile of the 38 second pulsar as a function of energy. No pulsation is detected in the data at energies above 80 keV.